

# Green Chemistry

Accepted Manuscript



This is an *Accepted Manuscript*, which has been through the Royal Society of Chemistry peer review process and has been accepted for publication.

*Accepted Manuscripts* are published online shortly after acceptance, before technical editing, formatting and proof reading. Using this free service, authors can make their results available to the community, in citable form, before we publish the edited article. We will replace this *Accepted Manuscript* with the edited and formatted *Advance Article* as soon as it is available.

You can find more information about *Accepted Manuscripts* in the [Information for Authors](#).

Please note that technical editing may introduce minor changes to the text and/or graphics, which may alter content. The journal's standard [Terms & Conditions](#) and the [Ethical guidelines](#) still apply. In no event shall the Royal Society of Chemistry be held responsible for any errors or omissions in this *Accepted Manuscript* or any consequences arising from the use of any information it contains.



[www.rsc.org/greenchem](http://www.rsc.org/greenchem)

# Catalytic fast pyrolysis of biomass: the reactions of water and aromatic intermediates produces phenols

Calvin Mukarakate,<sup>\*a</sup> Josefine D. McBrayer,<sup>b</sup> Tabitha J. Evans,<sup>a</sup> Sridhar Budhi,<sup>a,d</sup> David J. Robichaud,<sup>a</sup> Kristiina Iisa,<sup>a</sup> Jeroen ten Dam,<sup>c</sup> Michael J. Watson,<sup>c</sup> Robert M. Baldwin<sup>a</sup> and Mark R. Nimlos<sup>a</sup>

<sup>a</sup>National Bioenergy Center, National Renewable Energy Laboratory, 15013 Denver West Parkway, Golden, CO 80401-3393

<sup>b</sup>Department of Chemical and Biological Engineering, University of New Mexico, Albuquerque, NM 87131

<sup>c</sup>Johnson Matthey Technology Centre, PO Box 1, Belasis Avenue, Billingham, Cleveland, TS23 1LB, UK

<sup>d</sup>Department of Chemistry and Geochemistry, Colorado School of Mines, Golden, CO 80401

## Abstract

During catalytic upgrading over HZSM-5 of vapors from fast pyrolysis of biomass (ex situ CFP), water reacts with aromatic intermediates to form phenols that are then desorbed from the catalyst micropores and produced as products. We observe this reaction using real time measurement of products from neat CFP and with added steam. The reaction is confirmed when <sup>18</sup>O-labeled water is used as the steam source and the labeled oxygen is identified in the phenol products. Furthermore, phenols are observed when cellulose pyrolysis vapors are reacted over the HZSM-5 catalyst in steam. This suggests that the phenols do not only arise from phenolic products formed during the pyrolysis of the lignin component of biomass; phenols are also formed by reaction of water molecules with aromatic intermediates formed during the transformation of all of the pyrolysis products. Water formation during biomass pyrolysis is involved in this reaction and leads to the common observation of phenols in products from neat CFP. Steam also reduces the formation of non-reactive carbon in the zeolite catalysts and decreases the rate of deactivation and the amount of measured “coke” on the catalyst. These CFP results were obtained in a flow microreactor coupled to a molecular beam mass spectrometer (MBMS), which allowed for real-time measurement of products and facilitated determination of the impact of steam during catalytic upgrading, complemented by a tandem micropyrolyzer connected to a GCMS for identification of the products.

Corresponding author: calvin.mukarakate@nrel.gov

## 1. Introduction

Biomass has the potential to displace fossil fuels for the production of transportation fuels. This renewable resource can mitigate the negative impacts of using fossil fuels including the increase of greenhouse gases such as CO<sub>2</sub> in the atmosphere. Pyrolysis of biomass materials produces high yields of bio-oils (up to 75 wt%);<sup>1</sup> however, these oils have high oxygen contents (35-45 wt%) which contributes to several undesirable characteristics including acidity, instability, low heating value, and immiscibility with hydrocarbons.<sup>1-6</sup> The quality of bio-oil can be improved by catalytic fast pyrolysis (CFP) in order to remove oxygen prior to condensation. During ex situ CFP, primary vapors from pyrolysis are passed over catalysts at elevated temperatures to reject oxygen from the pyrolysis products in the form of water, CO, and CO<sub>2</sub>.<sup>7</sup> HZSM-5 has been widely studied as a catalyst for the CFP process largely due to its ability to almost completely deoxygenate pyrolysis products to form olefins and aromatic hydrocarbons.<sup>8-38</sup> However, the commercialization of CFP with HZSM-5 has been hampered by low yields of hydrocarbons, because large amounts of carbon are lost through formation of light gases and excessive coking of the catalyst. Catalyst coking also results in fouling and rapid deactivation, which means that the catalyst will require frequent regeneration and/or replenishment. In order to minimize coke formation and thus improve hydrocarbon yields, it is important to find methods and conditions that optimize the HZSM-5 CFP process; one option is introduction of steam. Steam is commonly employed in catalytic cracking units in petroleum refineries, where it is used for stripping hydrocarbons from spent catalysts (steam stripping), and for decreasing the partial pressure of hydrocarbons at the feed injection point in order to increase the feed vaporization rate (feed dispersion steam) and to reduce the rate of coking.<sup>39, 40</sup>

In an early study, canola oil was co-fed with steam over a fixed bed of HZSM-5<sup>41</sup> resulting in an increase in the yield of organics and a reduction in the amount of coke deposited on the catalyst compared to the same experiment conducted without steam. This resulted in a two-fold increase in the catalyst lifetime. Product analysis showed that addition of steam led to

a reduction in formation of deoxygenated aromatics and an increase in olefin and phenols production. The decrease in aromatic formation was attributed to partial decoupling of aromatization reactions from olefin formation. Similar results were also observed during upgrading of wood derived bio-oil,<sup>42</sup> upgrading of canola oil to hydrocarbons,<sup>43</sup> conversion of ethanol,<sup>44</sup> and conversion of furan,<sup>45</sup> all over HZSM-5 in the presence of steam. The selectivity for organic liquids was also greatly influenced by the weight hourly space velocity (WHSV).<sup>43</sup> The results showed that low WHSV increased the selectivity for organic liquids in the absence of added steam while a high WHSV increased the selectivity for organic liquids for experiments conducted with added steam.

Higher organic liquid yields were also produced during catalytic upgrading of pyrolysis vapors from perennial shrubs using a non-zeolite catalyst (Co-Mo) when the experiment was performed in the presence of steam.<sup>46</sup> Steam also improved the organic yields on other non-zeolite catalysts such as Al<sub>2</sub>O<sub>3</sub><sup>47</sup> and silica supported transition metals (Ni and V).<sup>48</sup> Co-feeding biomass with steam over Al<sub>2</sub>O<sub>3</sub> gave lower paraffin and phenol formation, but enriched ketones and organic acids. Silica-supported Ni and V catalysts formed higher amounts of phenols when co-fed with steam, with the V catalysts showing increased selectivity towards simple phenols instead of catechols. Addition of steam also improved both the quality and quantity of the organic liquids during catalytic upgrading of vapors from cottonseed cake using a natural zeolite.<sup>49</sup>

In an effort to combine the advantages realized from co-feeding steam with metal-based and zeolite catalysts, another study investigated the effect of steam on catalytic upgrading of biomass pyrolysis vapors using metal modified HZSM-5. The acidity of the catalyst was also varied by changing the zeolite to binder ratio. The combination of nickel-vanadium metals and HZSM-5 provided enhanced catalytic activity toward production of deoxygenated liquid while preserving or increasing the H/C ratio.<sup>50</sup> The acidic function of the catalyst deoxygenated carboxylic acids and carbonyls, and the metal functions were found to selectively deoxygenate phenols and methoxyphenols. This bi-functional

catalyst also formed less deoxygenated aromatic hydrocarbons, especially naphthalene and indene, in the presence of steam, which was attributed to steam decreasing the reaction rates for cyclization and condensation. It was also suggested that the competitive steam adsorption on the acid sites of the zeolite lowered the conversion to aromatics via Diels Alder cyclization of olefins, while high acid sites, at higher zeolite loading, promoted the cyclization of the produced olefins. Recently, the CFP of cellulose was studied in a fluidized-bed reactor.<sup>51</sup> The fluidizing gas consisted of He and/or steam at various vapor fractions of steam. Initially, the catalyst was pretreated with steam. This changed the structure of the catalyst leading to reversible and irreversible changes; for example dealumination, reduced total acidity, and agglomeration of particles. Co-feeding steam with cellulose reduced yields of aromatics and amount of coke deposits. However it increased the yields of unidentified carbon. The studies above show that steam has some positive impacts on CFP in terms of coke reduction and improving catalyst lifetime. However these studies did not give clear explanations why addition of steam reduced the formation of deoxygenated aromatics and coke deposits on the catalyst.

We hypothesize that steam reacts with aromatic precursors on zeolite active sites to form phenols. To the best of our knowledge, we have not seen any published work on formation of phenols from hydroxylation of aromatics with water using HZSM-5. Previous studies reported formation of phenol from direct hydroxylation of benzene with  $N_2O$  using HZSM-5.<sup>52-56</sup> In this reaction,  $N_2O$  molecule decomposes on specific areas of HZSM-5 to form molecular nitrogen and surface oxygen called  $\alpha$ -oxygen. The  $\alpha$ -oxygen will then react with benzene to form phenol.<sup>54</sup> It has been proposed that the  $\alpha$ -oxygen is created on the structural defects of the HZSM-5 framework.<sup>55, 56</sup> It was also shown that mild steaming of HZSM-5 increases these defects due to dealumination, and this led to an increase in the activity of HZSM-5 during hydroxylation of benzene with  $N_2O$ .<sup>52</sup> Cresols and naphthols were also observed during direct hydroxylation of alkyl benzenes and naphthalene with  $N_2O$  using HZSM-5.<sup>52</sup> Other studies have also reported formation of

phenol by direct hydroxylation of benzene with  $H_2O_2$  using non-zeolite based catalysts,  $CuFe_2O_4$ ,<sup>57</sup>  $FePO_4$ ,<sup>58</sup> and metal/graphene oxide<sup>59</sup>.

In this study we investigated the effects of steam on the yield of aromatic hydrocarbons, coke deposits, and formation of phenols during ex situ CFP of biomass using HZSM-5 as the catalyst. Reaction pathways that may lead to formation of phenols are proposed and their effect on aromatics and coke are discussed. We investigated the effect of co-feeding steam with discrete amounts of biomass to monitor the release of upgraded products in real-time, and we also conducted steam stripping experiments to see if any differences in product distributions were observed. The real-time experiments were conducted using pyrolysis molecular beam mass spectrometry (py-MBMS).<sup>7, 60</sup> Pyrolysis gas chromatography mass spectrometry coupled to a flame ionization detector (py-GCMS/FID) was used to complement the real-time runs.

## 2. Experiments

Experiments were primarily conducted using the py-MBMS system; this apparatus allows for real-time measurements of the products formed during the catalytic upgrading process. In this instrument three different basic types of experiments were conducted to investigate the role of steam during CFP of biomass: 1) without steam addition, 2) co-feeding biomass with steam, and 3) alternating biomass feeding with steam (steam stripping). In addition, steam stripping experiments were conducted in the py-GCMS/FID to identify and quantify products. Coke on spent catalysts was measured using thermogravimetric analysis (TGA). The number of acid sites on fresh and spent catalyst samples was measured with  $NH_3$  temperature-programmed desorption (TPD).

### 2.1 Materials

The experiments were conducted using Avicel cellulose, lignin and pine. The Avicel cellulose was obtained from Sigma Aldrich and used without further purification. The milled wood lignin was

prepared at the National Renewable Energy Laboratory (NREL) from southern yellow pine using the Björkman method.<sup>61</sup> The southern yellow pine supplied by Idaho National Laboratory (INL) was used in powdered form (less than 120  $\mu\text{m}$ ). The results from elemental analysis of southern yellow pine gave 52 % carbon, 41 % oxygen, 6 % hydrogen and less than 1 % nitrogen. The moisture content was 2.9 %. The HZSM-5 catalyst (silica binder) was supplied by Johnson Matthey (JM) (one millimeter particle sizes) and it had a silica-to-alumina ratio (SAR) of 30. The steam experiments were conducted using in-house DI water and  $^{18}\text{O}$  labelled water from Cambridge Isotope Laboratories (97% purity of  $^{18}\text{O}$ ).

## 2.2 Horizontal Reactor-MBMS

A detailed description of the laboratory reactor set-up can be found elsewhere.<sup>7, 60</sup> Briefly, powdered samples of biomass were pyrolyzed in the inner tube of an annular reactor and the evolved vapors were entrained and transported in helium carrier gas through a fixed catalyst bed. After the fixed catalyst bed, the upgraded products were then sampled and measured by the MBMS. The pyrolysis and upgraded products in the inner tube were transported by 0.4 slm of helium. This was further diluted with a 4 slm helium stream from the outer tube in order to dilute the products and minimize secondary reactions before the vapor stream was sampled by the MBMS orifice. Steam was co-fed with He in the inner tube at 0.06 ml/min using a syringe pump (NE-1000, New Era, Pump Systems Inc.). This translated to a steam-to-biomass ratio of 2.4. The annular reactor was heated to 500  $^{\circ}\text{C}$  using a five-zone furnace.<sup>7</sup>

The catalyst bed was prepared by weighing one gram of HZSM-5 and supporting it inside the inner tube at both ends with quartz wool. The reliability of the bed was tested by measuring the pressure drop across the bed both at room temperature ( $\sim 1$  torr) and at operational temperature ( $\sim 6$  torr). During an experiment, samples containing 50 mg of biomass were introduced at a rate of approximately one every four minutes into the pyrolysis zone of the inner tube, which was maintained at 500  $^{\circ}\text{C}$ . As will be discussed below, pyrolysis and upgrading of the evolved vapors took place over a two minute time

period and an additional two minutes were employed to allow species with low kinetic mobility to diffuse out of the HZSM-5 pores. Steam was either flowed continuously (co-fed) or alternated with biomass feeding (catalyst stripping). Up to approximately 25 samples were consecutively pyrolyzed during a typical experiment using a fixed bed of 1.0 g HZSM-5 catalyst. The weight hourly space velocity for these experiments was estimated to be about 4  $\text{h}^{-1}$ . The catalytically upgraded products from each periodic addition of biomass were sampled continuously by the MBMS orifice.

The MBMS<sup>7, 18, 19, 60, 62-64</sup> has been extensively used for direct, real-time measurements of products from biomass pyrolysis and CFP. This instrument allows universal detection and measurement of the entire complex suite of molecules produced during CFP. Molecular beam sampling is effective for direct measurements from hot, dirty environments with very good time resolution (c.a. 1 second), which allows for direct monitoring of coke precursors. Further, the adiabatic cooling of the molecular beam and the low ionization energy (22.5 eV) greatly reduces fragmentation and simplifies the spectra of the upgraded products. The main disadvantage of the MBMS is that it is difficult to distinguish different ions with the same nominal mass. This ambiguity is resolved by using complementary GCMS data to identify key products. Further details on measurement of products using the MBMS can be found elsewhere.<sup>7, 18, 19, 60, 62-64</sup>

## 2.3 Tandem micropyrolyzer-GCMS/FID

The results obtained from py-MBMS were complemented and validated by py-GCMS/FID. A detailed description of the tandem micropyrolyzer-GCMS can be found elsewhere.<sup>7</sup> Briefly, the micropyrolyzer (Rx-3050TR, Frontier Laboratories, Japan) has a pyrolysis zone and a catalytic upgrading zone, with the catalytic upgrading zone located downstream of the pyrolysis zone. The system is equipped with an autosampler (AS-1020E) and a microjet cryo-trap (MJT-1030Ex) coupled to the GCMS/FID, which was used to quantify and identify CFP products. Deactivated stainless steel cups containing 500  $\mu\text{g}$  biomass were loaded into the

autosampler. The cups were dropped into the pyrolysis zone maintained at 500 °C and the pyrolyzed vapors passed through the fixed catalyst bed (at 500 °C) for upgrading. The upgraded vapors were subsequently captured using a liquid nitrogen trap (set at -80 °C, housed inside the GC oven) and desorbed into the inlet of the gas chromatograph (7890B, Agilent Technologies, USA) interfaced with the MS (5977A, Agilent Technologies, USA). The trapped gases were separated by a capillary column (Ultra Alloy-5, Frontier Laboratories, Japan) with a 5 % diphenyl and 95 % dimethylpolysiloxane stationary phase. The oven was programmed to hold at 40 °C for 3 min followed by heating to 300 °C at the ramp rate of 10 °C min<sup>-1</sup>. Steam stripping experiments were conducted only in the py-GCMS/FID system. During the steam stripping studies, four samples of biomass were pyrolyzed sequentially and upgraded over a fixed catalyst bed (20 mg). This was followed by injecting 0.2 µl of water into the pyrolysis zone to form steam which in turn passed through the catalyst bed to remove carbonaceous deposits on the catalysts.

The products recorded on the mass spectrometer were identified using standards and NIST GCMS library. The py-GCMS/FID was calibrated for 42 compounds consisting of hydrocarbons and oxygenates detected during CFP of biomass. Response factors for non-calibrated compounds were selected based on the closest compound. The carbon yields of organic vapors were calculated by adding up the carbon detected in each compound and dividing by carbon in the biomass.

#### 2.4 NH<sub>3</sub> temperature-programmed desorption (TPD)

The NH<sub>3</sub>-TPD was conducted to measure the number of acid sites on fresh and spent catalyst samples. The measurements assumed a stoichiometry of one mole NH<sub>3</sub> molecule per acid site. The samples (200 mg) loaded in a quartz U-tube were measured on a micro-flow reactor (AMI-390) containing a thermal conductivity detector.<sup>7</sup> In this system, samples were pretreated by heating in 10 % O<sub>2</sub>/Ar (fresh) or Ar (spent) to 500 °C, hold for 60 min, and then cool to 120 °C in He flow and then perform the adsorption

step. The spent catalysts were not pretreated in O<sub>2</sub> to prevent removal of carbon by combustion. The adsorption step was achieved by flowing 10 % NH<sub>3</sub>/He for 30 min at 120 °C, followed by flushing with He. The TPD was performed by heating at 30 °C/min from 120-500 °C, with a 30 min hold at 500 °C. The gas flow rate in all steps was 25 sccm. The TCD was initially calibrated using a sample loop of known volume prior to quantification of the amount of NH<sub>3</sub> desorbed from the samples

#### 2.5 Coke Analysis

The amount of coke deposited on the catalyst was measured by thermogravimetric analysis (TGA) in a TGA Setaram (TN688, SETSYS Evolution) analyzer. The spent catalysts were heated in air at 20 °C/min from 25 °C to 780 °C. Two distinct mass loss peaks were observed and the mass loss from 250 to 650 °C was attributed to coke while that below 250 °C was associated with water and weakly adsorbed organic species. A control test was performed with fresh catalyst to ascertain that there was no mass loss in the fresh catalyst in the coke region.

### 3. Results and Discussion

#### 3.1 Py-MBMS

Upgrading of biomass pyrolysis vapor over HZSM-5, in the presence of steam, was found to enhance formation of phenol and alkyl phenols, and naphthol and alkyl naphthols. Our data shows that steam inhibits formation of polyaromatics, especially naphthalene and alkyl naphthalenes. Fig. 1 shows ion traces for selected aromatic hydrocarbons produced during CFP of pine using HZSM-5. Each pulse was produced from CFP of samples containing 50 mg pine. The products from CFP of the first sample gave the mass spectrum shown in Fig. 2A. This mass spectrum was developed by averaging over the main pulse from time = 2 to 4 minutes in Fig. 1 (note that there is a tail of products from 4 to 7 minutes), and it contains species that can be assigned to benzene and alkyl benzenes (m/z 78, 91, 106, 120), naphthalene and alkyl naphthalenes (m/z 128, 142, 156, 170) and anthracene and alkyl anthracenes (m/z 178, 192, 206) as shown in Table 1. These species have been observed and reported during catalytic upgrading of

biomass vapors and bio-oil using HZSM-5 in several previous publications.<sup>8-10, 16, 19, 20, 60, 65</sup>

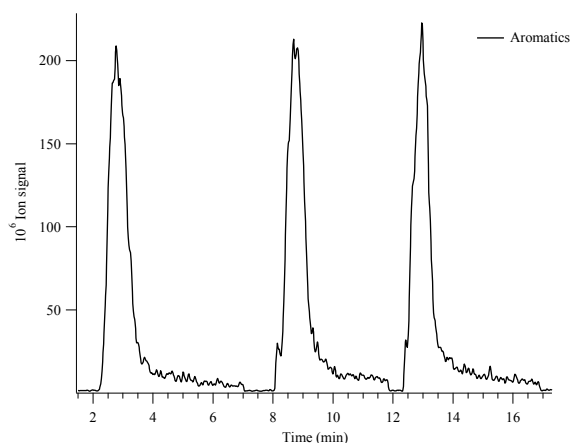


Fig. 1. Ion signals for selected aromatic hydrocarbons from upgrading pine pyrolysis products with HZSM-5 at 500 °C, each pulse was obtained from CFP of 50 mg of pine. Note that there is a tail of products after each pulse.

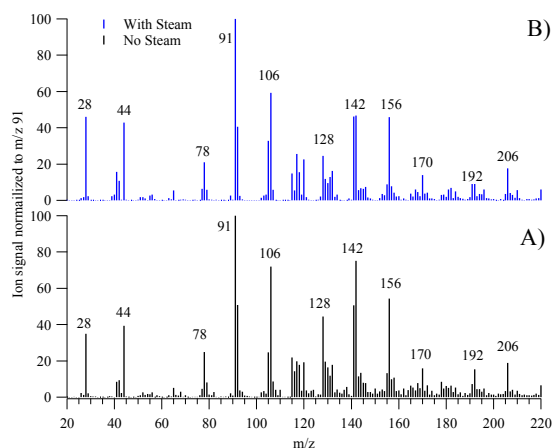


Fig. 2. Comparison of mass spectra from pulse 1 (time 2-4 minutes) recorded A) without steam and B) with steam. The mass spectra are normalized to the most intense peak ( $m/z$  91)

Table 1. Compounds observed by MBMS during vapor phase upgrading of biomass pyrolysis products using HZSM-5.

$m/z$	Compound	$m/z$	Compound
-------	----------	-------	----------

18	Water	122	Dimethyl phenols
28	Carbon monoxide	128	Naphthalene
44	Carbon dioxide	132	Methyl indane
78	Benzene	142	Methyl naphthalenes
91	Toluene	144	Naphthols
94	Phenol	156	Dimethyl naphthalenes
106	Xylenes and ethyl benzenes	158	Methyl naphthols
108	Methyl phenols	170	Trimethyl naphthalenes
116	Indene	178	Anthracene
118	Indane	192	Methyl anthracenes
120	Trimethyl benzenes and methyl ethyl benzenes	206	Dimethyl anthracenes

A second experiment in which pine was co-fed with steam was conducted, and the mass spectrum averaged from the analogous main pulse in Fig. 2B shows that there were no major differences in the product composition. However, the intensities for naphthalenes ( $m/z$  128, 142, 156) relative to the benzenes ( $m/z$  78, 91, 106) are lower in the case where biomass was co-fed with steam. This suggests that steam was inhibiting the formation of polyaromatic hydrocarbons as reported earlier.<sup>42, 43, 48, 50</sup> Mass spectra were also recorded for the tails after the pulses, for example the tail of pulse 1 from Fig. 1 was averaged from time = 4 to 7 minutes and it produced the mass spectrum shown in Fig. 3A. This spectrum shows that the composition of products between the main pulse (Fig. 2A) and tail are similar for the experiment conducted without steam. There is a significant difference however in the distribution of the products; polyaromatics become more intense relative to the benzene and alkyl benzenes. This is likely due to the polyaromatic hydrocarbons having lower kinetic mobility inside the pores compared to the less bulky one-ring aromatics. When this

experiment was conducted with steam, new intense peaks were observed in the tail of the pulse; those peaks are labelled in red in Fig. 3B. These species can be assigned to phenol and alkyl phenols ( $m/z$  94, 108, 122) and naphthol and alkyl naphthols ( $m/z$  144, 158, 172) as shown in Table 1 (Table S1 shows the structure of these compounds). The peaks at  $m/z$  66 and 115 are fragment ions of phenol and naphthol respectively. The observation of phenols in the tail and not in the pulse could be due to the fact that phenols are polar, which may cause these molecules to be tightly held on active sites in the catalyst pores compared to the nonpolar aromatic compounds, such as benzene.<sup>60</sup> Experiments conducted by passing a mixture of naphthalene and phenol over HZSM-5 at 500 °C provided further evidence that phenol is retained in the catalyst and addition of steam helps push it out of the pores.

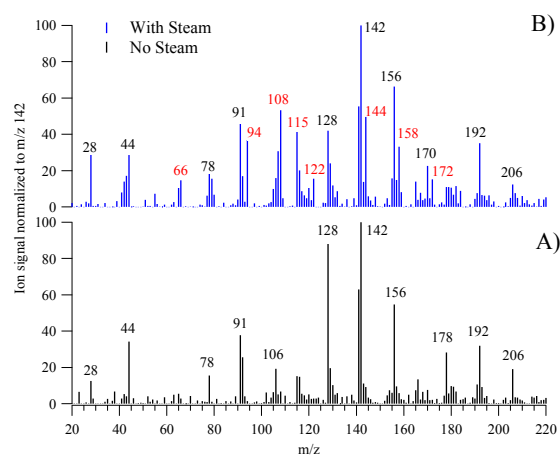


Fig. 3. Comparison of mass spectra from the tail after pulse 1 (time 4-7 minutes) recorded A) without steam and B) with steam.

Fig. 4 shows the sum of yields of selected products observed with each subsequent sample pyrolyzed. The yields were estimated by integrating the ion signals for the MBMS peaks. The sum of peaks at  $m/z$  78, 91 and 106, represents benzene, toluene and xylenes, while the peaks at  $m/z$  94, 108, 122 and 158, likely represent phenol, methyl phenol, dimethyl phenol and methyl naphthol which all became more intense during experiments conducted with steam. As can be seen in Fig. 4A, the integrated signals of benzene and alkyl benzenes are increased by steam.

The catalyst lifetime is also improved because these species are still being produced even at high biomass-to-catalyst ratios ( $> 0.8$ ). In contrast, the yields of these species are almost zero at corresponding biomass-to-catalyst ratios for the experiment conducted without steam.

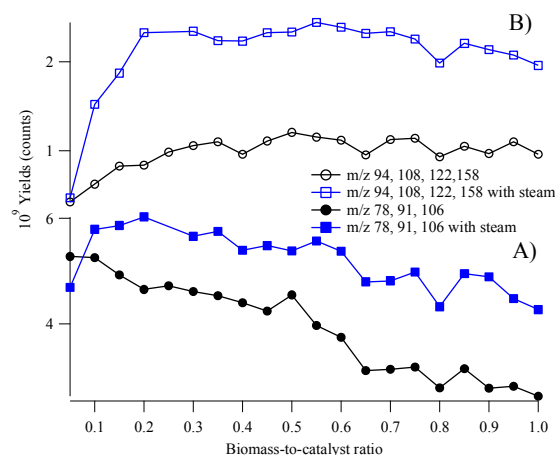


Fig. 4. Integrated ion signals (yields) of selected mass spectral peaks from Fig. 3 during CFP of 20 samples, each containing 50 mg of pine, and the vapors passed over a fixed bed containing 1.0 g HZSM-5. The pulses in (A) are for benzene and alkyl benzenes, and the pulses in (B) are for phenols and methyl naphthol, which are enhanced by steam.

Fig. 4B shows that steam increases the yields of phenols and naphthols. Initially, small amounts of these species are observed and without added steam the integrated signals of these species increases gradually up to a biomass-to-catalyst ratio of 0.35, where the signals stay constant for the remainder of the experiment. This increase is likely due to an increase in hydrocarbon species trapped in the pores of the catalyst. These species are released from the catalyst pores by steam produced by dehydration reactions during pyrolysis of subsequent pine samples. When the experiment was conducted with steam, the phenols and naphthols sharply increased to a maximum at a biomass-to-catalyst ratio of 0.2, and then remained constant for the rest of the experiment.

To understand the production of single- vs multi-ring aromatics, we summed the estimated yields from

integrated signals of benzenes ( $m/z$  78, 92, 106) and phenols and naphthols ( $m/z$  94, 108, 122, 158) during CFP of the 20 samples (biomass-to-catalyst ratio 1.0) shown in Fig. 4. The experiment conducted without steam produced  $7.9 \times 10^{10}$  counts of benzenes and the steam experiment produced  $1.0 \times 10^{11}$  counts, indicating that steam increased the amount of one-ring aromatic hydrocarbons by 31 %. The phenols and alkyl naphthols ( $m/z$  94, 108, 122, 158) increased from  $2.0 \times 10^{10}$  to  $4.1 \times 10^{10}$  counts, an increase of 109 %. Similar estimates for yields of deoxygenated two-ring aromatic hydrocarbons ( $m/z$  128, 142, 156) in Fig. S1B (supplementary information) show that steam increased these species from  $5.6 \times 10^{10}$  to  $5.8 \times 10^{10}$  counts. This represents a mere 4 % increase, which is less than that of benzenes. Since both one-ring and two-ring aromatic hydrocarbons are formed from the same reaction mechanisms as predicted by the “hydrocarbon pool” chemistry,<sup>66, 67</sup> steam could be inhibiting formation of multi-ring aromatics. Fig. S1A shows data for estimating the yields of olefins (propylene  $m/z$  42 and butenes  $m/z$  56), which was increased by steam from  $8.5 \times 10^9$  to  $1.5 \times 10^{10}$  counts (75 %). These results indicate that steam inhibits formation of polyaromatics and promotes formation of benzenes, olefins, phenols and naphthols.

Could the increase in phenols and naphthols be because steam is preventing complete deoxygenation of pyrolysis vapor, or is it reacting with some hydrocarbon intermediates in the catalyst pores? To evaluate how the phenols and naphthols are formed, we conducted another experiment, where we alternated feeding biomass with feeding steam (steam stripping). Steam was introduced only after the signal from the upgraded products was zero as shown in Fig. S2. The spectrum in Fig. 5A was obtained during steam stripping of HZSM-5 after pyrolysis of three pine samples, and it contains aromatic hydrocarbons, phenols and naphthols as was found in the tail of the pulse in experiments conducted with steam shown in Fig. 3B above. This indicates that steam was not preventing complete deoxygenation of pyrolysis vapors. The major difference from Fig. 3B is that the intensities of phenols and naphthols are higher than those of the aromatics. This is because the spectrum in Fig. 5A was recorded after CFP of the third sample

(see Fig. S2) compared to just after CFP of the first sample in Fig. 3B. This suggests that the species that result in phenols and naphthols build up inside the catalyst pores as the catalyst ages.

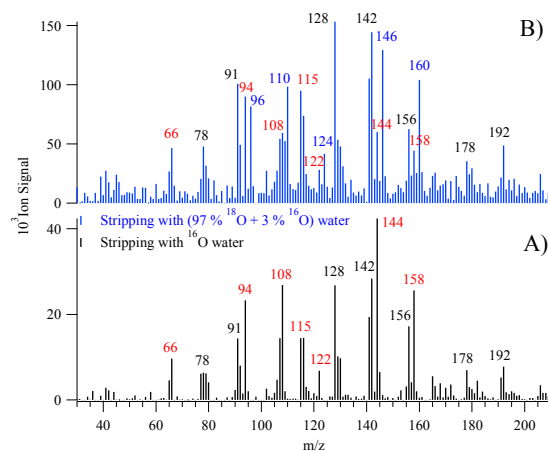


Fig. 5. The spectra recorded from stripping HZSM-5 with steam after passing three samples of 50 mg pine A)  $^{16}\text{O}$  water and B) (97 %  $^{18}\text{O}$  + 3 %  $^{16}\text{O}$ ) water

A similar experiment with  $^{18}\text{O}$ -labeled water was performed to ascertain if steam (water) was participating as a chemical reactant. Fig. 5B shows the spectrum that was recorded during steam stripping of HZSM-5 using water containing 97%  $^{18}\text{O}$ , and it shows that phenol and alkyl phenols and naphthol and alkyl naphthols contain both  $^{16}\text{O}$  and  $^{18}\text{O}$ , suggesting that phenols and naphthols are likely formed from reactions of water with hydrocarbon intermediates in the catalyst pores. The oxygenated aromatic hydrocarbons from  $^{16}\text{O}$  are labeled in red, and they include phenol  $m/z$  94, methyl phenols  $m/z$  108, dimethyl phenols  $m/z$  122, naphthol  $m/z$  144 and methyl naphthols  $m/z$  158. The corresponding oxygenated aromatic hydrocarbons formed from  $^{18}\text{O}$ -labeled steam are in blue, and they include phenol  $m/z$  96, methyl phenols  $m/z$  110, dimethyl phenols  $m/z$  124, naphthol  $m/z$  146, and methyl naphthols  $m/z$  160. The presence of  $^{18}\text{O}$ -labeled products confirms that steam is participating as a chemical reactant to form phenols and naphthols. It is interesting to note that anthrols ( $m/z$  194, 208) were not observed in this experiment. This could be due to steric hindrances in the catalyst pores.

The steam used in this experiment contained only 3 %  $^{16}\text{O}$ , but Fig. 5B shows intense peaks for species associated with  $^{16}\text{O}$ ,  $m/z$  94, 108, 144 and 158. This could be because all the hydroxyl groups did not originate from the steam addition. To evaluate this observation, we plotted the variation of both  $^{16}\text{O}$  and  $^{18}\text{O}$ -labeled steam with time. As can be seen in Fig. 6A, an initial big pulse of  $^{16}\text{O}$  steam is observed, which decreases and levels off with time. The extra  $^{16}\text{O}$  steam could be coming from water formed during CFP of biomass samples, which was trapped in the micropores of the catalyst. In contrast, the  $^{18}\text{O}$  steam increases rapidly to a maximum and levels off with time. Fig. 6B shows that most phenols and naphthols are initially formed from the reaction of the  $^{16}\text{O}$  steam with aromatic species, which could be due to the catalyst surface being initially covered by  $^{16}\text{O}$  water, which reacts more readily. The products from the  $^{18}\text{O}$  steam are seen to dominate the spectrum after the  $^{16}\text{O}$  steam levels off or have been consumed to produce phenols and naphthols. This is clearly shown in Fig. 7, which shows mass spectra collected after averaging at three time intervals labeled X, Y, and Z in Fig. 6.

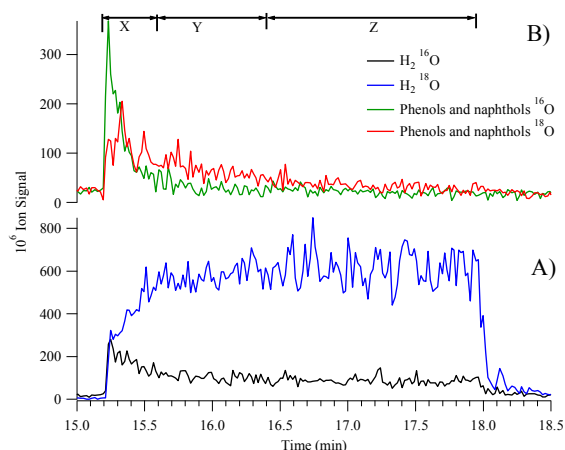


Fig. 6. Ion count profiles recorded when steam (97 %  $^{18}\text{O}$  + 3 %  $^{16}\text{O}$ ) was passed over spent HZSM-5, A) steam and B) phenol and naphthols. X, Y and Z represent time intervals shown in Fig. 7.

As can be seen in Fig.7A, the mass spectrum recorded at time interval X (from Fig. 6) contains intense peaks for phenols and naphthols formed from the  $^{16}\text{O}$  steam. However, the spectrum recorded at

time interval Y, Fig 7B, shows that the phenols and naphthols are formed from reactions of the  $^{18}\text{O}$  steam and there are almost no detectible oxygenated compounds formed from the  $^{16}\text{O}$  steam. Note that the fragment ions in Fig. 7 at  $m/z$  66 and 115 do not contain oxygen (Figs. 7A and 7B). The aromatic hydrocarbons, especially naphthalene and alkylated naphthalenes with low kinetic mobility, begin to dominate the spectrum towards the end of the steam pulse at time interval Z (Fig 7C). These aromatics are removed from the catalyst through steam stripping and could eventually form graphitic coke if they are not removed from the catalyst pores.

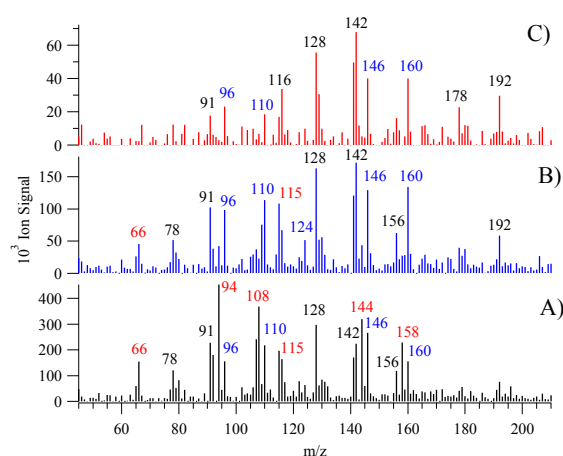


Fig. 7. Mass spectra recorded after passing steam (97 %  $^{18}\text{O}$  + 3 %  $^{16}\text{O}$ ) over spent HZSM-5 at time intervals A) X, B) Y, and C) Z in Fig.6. Masses labeled in red are for species with  $^{16}\text{O}$  and those in blue are species with  $^{18}\text{O}$ .

One possibility for the observation of phenols could be that they originate from lignin pyrolysis products, which condense on the catalyst surface. The lignin products will then react with steam to form phenols. Phenols and cresols are formed from non-catalytic pyrolysis of lignin and biomass as reported in previous work.<sup>18, 68, 69</sup> In order to show that the phenols and naphthols observed during CFP of pine were not produced from pyrolysis of the lignin component of pine, the  $^{16}\text{O}$ -steam stripping experiment was also conducted using lignin and cellulose. Fig. 8A shows mass spectra recorded from steam stripping of HZSM-5 after CFP of three samples of lignin. Fig. 8B was recorded from a

similar experiment after CFP of three samples of cellulose. These spectra show that phenols and naphthols are formed in both the cellulose and lignin experiments. Similar results were observed when these biopolymers were co-fed with steam. The observation of phenols and naphthols from cellulose in Fig. 8B provides additional evidence that these oxygenated aromatic species are produced in part by reaction of steam with aromatic species during catalytic upgrading and not from non-catalytic pyrolysis of lignin.

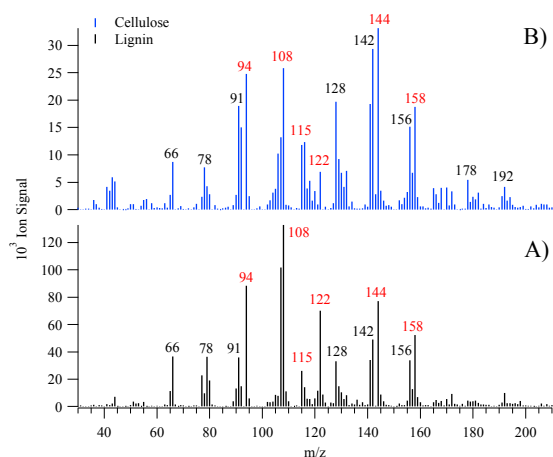


Fig. 8. Spectra recorded from stripping HZSM-5 with steam after passing three samples of 50 mg A) lignin and B) cellulose

Another experiment was conducted with cellulose and  $^{18}\text{O}$ -labeled water to ascertain if the initial observation of  $^{16}\text{O}$ -labeled products in Fig. 7A was due to the lignin component of pine. The ion count profiles in Fig. S3, also show the initial formation of phenols from  $^{16}\text{O}$ -labeled water as in Fig. 7A, confirming that the  $^{16}\text{O}$ -labeled products were not formed from the lignin component of pine. Experiments conducted by passing phenol over HZSM-5 and stripping off the catalyst with  $^{18}\text{O}$ -labeled water only produced  $^{16}\text{O}$  phenol. This indicates that no oxygen scrambling occurred during the biomass CFP experiments in Fig. 6 and 7.

This result shows that steam acts both as a reactant and a stripping agent. However, it does not provide enough evidence to reveal the nature of the aromatic

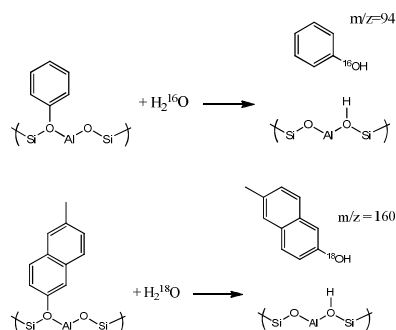
precursors in HZSM-5 pores which are actually reacting with steam to form phenols and naphthols or to determine whether the aromatic species are covalently or ionically bonded to the acid sites. Thus, it is impossible to use these results to unravel the actual reaction mechanisms for the formation of phenols; nevertheless, we can use the results and literature results for methanol-to-hydrocarbon conversion over HZSM-5 to propose possible reaction pathways.

Upgrading pine pyrolysis products over HZSM-5 produces similar products to upgrading methanol over HZSM-5 (methanol-to-hydrocarbons) as shown in Fig. S4. The only difference is that methanol produces large amounts of olefins and only one-ring aromatics. We can assume that the reaction mechanisms occurring during upgrading over HZSM-5 are similar for both pyrolysis vapors and methanol. Thus, the catalytic upgrading of pine pyrolysis products over HZSM-5 can be hypothesized to occur through the so-called hydrocarbon pool described for methanol-to-hydrocarbons.<sup>66, 67, 70</sup> The species in the hydrocarbon pool will react with pyrolysis vapors to form aromatic hydrocarbons, which then react with steam to form the phenols and naphthols. Both covalently<sup>71</sup> bonded and carbocations<sup>66, 67, 70</sup> species have been observed during the methanol-to-olefin studies. We therefore propose two possible pathways for the formation of phenols, scheme 1 and scheme 2.

An earlier study<sup>71</sup> reported that methanol reacts with acidic zeolites to form surface methoxy species (SMS), which act as intermediates for reaction with different probe molecules. The SMS consisted of a methyl group covalently bonded to an oxygen atom on the Si-O-Al bridge. If similar reactions were to occur in our study, this would mean that biomass vapors react with HZSM-5 to form surface phenyl species (SPS) and surface naphthyl species (SNS). These species could then react with steam to form phenols and naphthols as shown in Scheme 1.

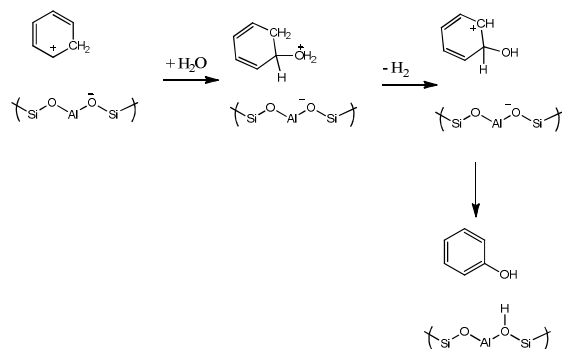
Fig. 7 shows results from an experiment which passed 97 %  $^{18}\text{O}$  plus 3 %  $^{16}\text{O}$  labelled steam over spent HZSM-5. Scheme 1 shows steam reacting with a surface phenyl species to produce phenol and regenerate an acid site. The m/z 94 phenol was

formed from reaction of  $^{16}\text{O}$ -labeled steam. Scheme 1 also shows the reaction of  $^{18}\text{O}$ -labeled steam with surface methyl naphthyl species to produce the  $m/z$  160 methyl naphthol and then regenerate an acid site. Other oxygenated aromatics shown in Fig. 7 could be formed via reaction pathways shown in Scheme 1.



Scheme 1

The aromatic species could also be ionically bonded to active sites. An earlier study investigated if biomass CFP proceeds through the hydrocarbon pool chemistry.<sup>36</sup> Mixtures of  $^{12}\text{C}$  and  $^{13}\text{C}$  glucose were pyrolyzed in the presence of HZSM-5 and the products observed consisted of random mixtures of  $^{12}\text{C}$  and  $^{13}\text{C}$  aromatic hydrocarbons. The observed carbon scrambling was attributed to the existence of the hydrocarbon pool intermediate. Accordingly, if reactions in our study occurred via the hydrocarbon pool chemistry then the phenols and naphthols are produced via the reaction pathway proposed in Scheme 2. This pathway shows presence of aromatic carbocations in zeolite pores, which reacts with steam to produce  $^{18}\text{O}$ -labeled phenol and regenerate an acid site.



Scheme 2

Another possibility could be that the hydroxyl groups from the zeolite framework react with the aromatic species to form phenols and naphthols. In this case, the oxygen in water will exchange with the framework oxygen as reported in a previous study.<sup>72</sup> It was shown that the oxygen in both Si-O-Al and Si-O-Si bridges of the zeolite was exchanged with oxygen from  $^{18}\text{O}$ -labeled water. This could mean that the  $^{18}\text{O}$  inserted on aromatic species in our data is initially exchanged with framework oxygen to form hydroxyl groups, which will then react with aromatic species to form phenol and naphthols. Additional experiments, possibly using model compounds are required to unravel the actual reaction mechanisms for the formation of phenols and naphthols in HZSM-5.

### 3.2 py-GCMS

A py-GCMS experiment was conducted to confirm the identity of the oxygenated aromatics stripped by steam. As we have discussed in our previous work,<sup>7, 60</sup> the GCMS has advantages over the MBMS system including the ability to distinguish structural isomers. The py-GCMS set-up does not allow co-feeding steam with biomass hence we can only conduct steam stripping experiments in this apparatus. Further, the GCMS system utilizes small biomass samples (0.5 mg), which is 100 times smaller than we use for the MBMS experiments. In order to have sufficient quantities of materials to strip from the catalyst, four samples of biomass were pyrolyzed and the products were measured using GCMS. Due to the GC analysis time it took 45 minutes to run each biomass sample and a total of three hours for the four samples. Water containing  $^{16}\text{O}$  and  $^{18}\text{O}$  was then injected in the reactor with the spent catalyst. Chromatograms from both the CFP and the steam stripping experiments are shown in Fig. 9. Fig. 9A was recorded during CFP of pine and it contains 1-3 ring aromatic hydrocarbons as reported earlier.<sup>14, 15, 25, 60, 65</sup> Fig. 9B was recorded from steam stripping experiments and contains peaks for phenols and naphthols - phenol, 3-methyl phenol, 2-methyl phenol, naphthol (2-naphthalenol), and 2-methyl naphthol (2-methyl, 1-naphthalenol). Fig. 9B also shows that deoxygenated aromatic hydrocarbons

are released during the steam stripping experiment and these include mainly naphthalene and alkyl naphthalenes and also limited quantities of anthracenes and benzenes. These results are in very good agreement with the MBMS study above.

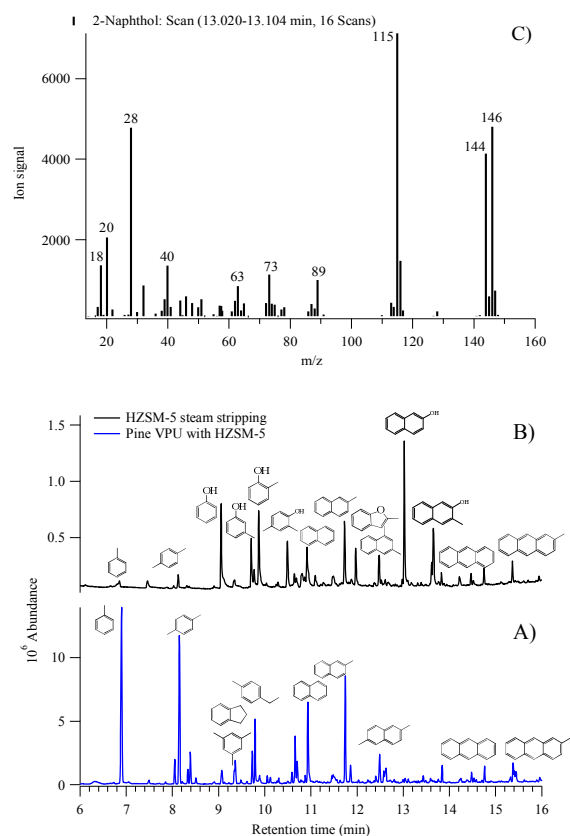


Fig. 9. Chromatograms recorded during pine CFP using HZSM-5. A) Upgrading pine pyrolysis vapors. B) Steam (97 %  $^{18}\text{O}$  + 3 %  $^{16}\text{O}$ ) stripping HZSM-5. C) Electron impact fragmentation pattern generated from 2-naphthalenol.

As can be seen, the formation of phenols and naphthols via reactions with steam was confirmed in the py-GCMS experiment. This can be seen from the fragmentation pattern generated from the peak of naphthol (2-naphthalenol), Fig. 9C, which has two parent peaks at  $m/z$  144/146 indicating that naphthol was formed from both  $\text{O}^{16}$  and  $^{18}\text{O}$  steam.

Table 2. The yields of condensable vapors from CFP of pine using HZSM-5 and steam stripping of the catalyst performed on the py-GCMS/FID system

	$\mu\text{g C}$ in vapors	C yield/ $\mu\text{g C}$ in vapors/ $\mu\text{g C}$ in biomass (%)
Sample 1	39.2	17
Sample 2	30.6	12
Sample 3	30.3	14
Sample 4	27.2	11
Steam	0.6	0.1 *

\* Per total biomass fed

Table 2 shows that the average carbon yield in condensable vapors measured for the four CFP experiments was 14%. Steam stripping released additional vapors corresponding to 0.1% carbon yield. Due to the GC analysis time it took 45 minutes to run each biomass sample and a total of three hours for the four samples. There was thus ample time for the carbonaceous deposits on the catalyst to mature into coke, which likely reduced the amount of organics released during the steam stripping stage. The low yield during these steam stripping experiments underscores that it is important to introduce steam immediately to remove the species from catalyst pores before they form polyaromatic hydrocarbons, which polymerize to form coke.

### 3.3 Effect of steam on coke formation

Coke deposits on the catalyst result in deactivation of HZSM-5. Our data shows that the addition of steam to the CFP process inhibits the formation of polyaromatic hydrocarbons, which are known to be potent coke precursors. To determine the impact of steam on coke formation spent catalysts were collected after pyrolysis and upgrading of 10 pine samples (0.5 g) using the py-MBMS system. Coke measurements were done on two spent catalysts: without steam and with co-feeding steam. The results from the analysis of the spent catalysts are shown in Table 3. The TGA analysis of the spent catalysts showed that co-feeding steam reduced the amount of coke deposited on the catalyst by 42 %. Measuring the total number of acid sites available on spent catalysts can also provide further proof for coke reduction. The  $\text{NH}_3$  TPD measurements of total acid sites shows that co-feeding steam with biomass resulted in a 22 % reduction in acid sites available for chemical reaction compared to 35 % reduction for experiments conducted without steam. These results indicate that steam reduced coke formation and thus

improves the lifetime of the catalyst because there are more acid sites accessible for chemical reaction compared to the no steam case. Additional evidence for reduced coke formation can be seen in Fig. 10, which shows estimate of yields of guaiacol  $m/z$  124, one of the pine pyrolysis products.<sup>18, 68</sup> Guaiacol breaks through immediately when the experiment is conducted without steam and it increases rapidly as more pine samples are pyrolyzed. This is because the catalyst is losing activity due to coke deposits. Co-feeding biomass with steam delays the breakthrough and reduces the amount of guaiacol formed after CFP of 10 samples.

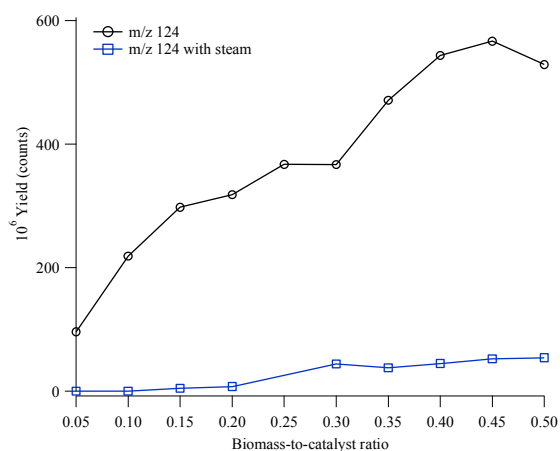


Fig. 10. Integrated ion signals (yields) of guaiacol  $m/z$  124 from CFP of pyrolysis of 10 samples, each containing 50 mg of pine, and the vapors passed over a fixed bed containing 1.0 g HZSM-5. The experiments were conducted without steam (black) and with steam (blue).

Table 3. The results from addition of steam to pine CFP using HZSM-5 performed on the py-MBMS system.

Experiment	No steam	Co-feeding Steam
Coke (wt %)	7.0	4.1
Total acid sites after CFP of 10 samples ( $\mu\text{mol/g}$ ) (fresh catalyst has 773 $\mu\text{mol/g}$ total acid sites)	501	631
Integration of one-ring aromatics after 10	4.7	5.4

samples ( $\times 10^{10}$  counts)

Integration of two-ring aromatics after 10 samples ( $\times 10^{10}$ counts)	3.4	3.4
Integration of phenols and naphthols after 10 samples ( $\times 10^9$ counts)	0.9	1.9

We also estimated the yields of one-ring and two-ring aromatics and phenols and naphthols after CFP of 10 samples. Integration of the ion signals from py-MBMS (Table 3) shows that co-feeding steam increased one-ring aromatic hydrocarbons by 15 % and olefins by 85 %. Steam had no effect on the yield of two-ring aromatic hydrocarbons; however, it increased yields of phenols and naphthols by 109 %.

#### 4. Conclusions

The following list summarizes important results from co-feeding steam with biomass and stripping spent catalyst with steam:

1. Fresh HZSM-5 upgrades biomass pyrolysis vapors to form aromatic hydrocarbons, and when steam is present some oxygenated aromatics are observed (phenol and alkyl phenols, naphthol and alkyl naphthols). Similar product speciation is also observed from steam stripping experiments. Small quantities of the oxygenated aromatics are also observed in studies conducted without steam. This is due to the moisture content of biomass and/or water produced from dehydration reactions.
2. Steam increased the yields of one-ring aromatics, olefins and phenol and alkyl phenols by inhibiting formation of polyaromatic hydrocarbons.
3. The studies conducted with  $^{18}\text{O}$ -labeled water reveal that the oxygen in water reacts with aromatic precursors to form phenol and alkyl phenols and naphthol and alkyl naphthols.
4. Steam reduces the amount of coke deposited on the catalyst by reacting with aromatic

hydrocarbons. This in turn improves the catalyst lifetime within a cycle by making more acid sites available for chemical reactions. However, steam has been shown to cause dealumination of the catalyst especially at high temperatures, which results in loss of catalyst activity after several cycles.<sup>51</sup> Addition of phosphorous to HZSM-5 has been demonstrated to prevent dealumination.<sup>51, 73</sup>

### Acknowledgements

This work was supported by the U.S. Department of Energy's Bioenergy Technologies Office (DOE-BETO) Contract No. DE-AC36-08GO28308 with the National Renewable Energy Laboratory and Johnson Matthey. JDM would like to thank DOE, Office of Science's Science Undergraduate Laboratory Internship program. The authors would like to thank Rui Katahira, Matthew Yung, Robert Evans and Kellene McKinney for stimulating discussions.

### References

1. A. V. Bridgwater, *Fast Pyrolysis of Biomass: A Handbook*, CPL Press, Newbury, UK, 1999.
2. A. V. Bridgwater, *Fast Pyrolysis of Biomass: A Handbook Volume 2*, CPL Press, Newbury, UK, 2002.
3. A. V. Bridgwater, *Fast Pyrolysis of Biomass: A Handbook Volume 3*, CPL Press, Newbury, UK, 2005.
4. A. Oasmaa, E. Leppamaki, P. Koponen, J. Levander and E. Tapola, in VTT Publications, 1997, vol. 306, pp. 1-87.
5. A. Oasmaa and C. Peacocke, in VTT Publications 2001, vol. 450, pp. 1-102.
6. A. Oasmaa and C. Peacocke, in VTT Publications 2010, vol. 731, pp. 1-134.
7. C. Mukarakate, M. J. Watson, J. ten Dam, X. Baucherel, S. Budhi, M. M. Yung, H. X. Ben, K. Iisa, R. M. Baldwin and M. R. Nimlos, *Green Chemistry*, 2014, **16**, 4891-4905.
8. J. D. Adjaye and N. N. Bakhshi, *Fuel Process. Technol.*, 1995, **45**, 161-183.
9. J. D. Adjaye and N. N. Bakhshi, *Fuel Process. Technol.*, 1995, **45**, 185-202.
10. F. A. Agblevor, S. Beis, O. Mante and N. Abdoulmoumine, *Ind. Eng. Chem. Res.*, 2010, **49**, 3533-3538.
11. F. A. Agblevor, O. Mante, N. Abdoulmoumine and R. McClung, *Energy Fuels*, 2010, **24**, 4087-4089.
12. E. Antonakou, A. Lappas, M. H. Nilsen, A. Bouzga and M. Stocker, *Fuel*, 2006, **85**, 2202-2212.
13. A. A. Boateng, C. A. Mullen, C. M. McMahan, M. C. Whalen and K. Cornish, *J. Anal. Appl. Pyrolysis*, 2010, **87**, 14-23.
14. T. R. Carlson, G. A. Tompsett, W. C. Conner and G. W. Huber, *Top. Catal.*, 2009, **52**, 241-252.
15. T. R. Carlson, T. R. Vispute and G. W. Huber, *Chemsuschem*, 2008, **1**, 397-400.
16. J. Diebold and J. Scahill, *ACS Symp. Ser.*, 1988, **376**, 264-276.
17. D. C. Elliott, *Energy Fuels*, 2007, **21**, 1792-1815.
18. R. J. Evans and T. A. Milne, *Energy Fuels*, 1987, **1**, 123-137.
19. R. J. Evans and T. A. Milne, in *Pyrolysis Oils from Biomass*, eds. E. J. Soltes and T. A. Milne, ACS Symposium Series, Washington, DC, 1988, ch. 26, pp. 311-327.
20. R. French and S. Czernik, *Fuel Process. Technol.*, 2010, **91**, 25-32.
21. A. G. Gayubo, A. T. Aguayo, A. Atutxa, B. Valle and J. Bilbao, *J. Chem. Technol. Biotechnol.*, 2005, **80**, 1244-1251.
22. A. G. Gayubo, B. Valle, A. T. Aguayo, M. Olazar and J. Bilbao, *Ind. Eng. Chem. Res.*, 2010, **49**, 123-131.
23. T. Q. Hoang, X. Zhu, T. Danuthai, L. L. Lobban, D. E. Resasco and R. G. Mallinson, *Energy Fuels*, 2010, **24**, 3804-3809.
24. P. A. Horne and P. T. Williams, *J. Anal. Appl. Pyrolysis*, 1995, **34**, 65-85.

25. C. A. Mullen, A. A. Boateng, D. J. Mihalcik and N. M. Goldberg, *Energy Fuels*, 2011, **25**, 5444-5451.
26. E. Putun, B. B. Uzun and A. E. Putun, *Energy Fuels*, 2009, **23**, 2248-2258.
27. S. D. Stefanidis, K. G. Kalogiannis, E. F. Iliopoulou, A. A. Lappas and P. A. Pilavachi, *Bioresour. Technol.*, 2011, **102**, 8261-8267.
28. M. J. A. Tijmensen, A. P. C. Faaij, C. N. Hamelinck and M. R. M. van Hardeveld, *Biomass Bioenergy*, 2002, **23**, 129-152.
29. B. Valle, A. G. Gayubo, A. T. Aguayo, M. Olazar and J. Bilbao, *Energy Fuels*, 2010, **24**, 2060-2070.
30. T. P. Vispute, H. Zhang, A. Sanna, R. Xiao and G. W. Huber, *Science*, 2010, **330**, 1222-1227.
31. S. Vitolo, B. Bresci, M. Seggiani and M. G. Gallo, *Fuel*, 2001, **80**, 17-26.
32. S. Vitolo, M. Seggiani, P. Frediani, G. Ambrosini and L. Politi, *Fuel*, 1999, **78**, 1147-1159.
33. P. T. Williams and N. Nugranad, *Energy*, 2000, **25**, 493-513.
34. A. H. Zacher, D. Santosa, D. C. Elliott and C. D. B. Brown, *TCBiomass 2011*, 2011.
35. H. Zhang, R. Xiao, H. Huang and G. Xiao, *Bioresour. Technol.*, 2009, **100**, 1428-1434.
36. T. R. Carlson, J. Jae and G. W. Huber, *Chemcatchem*, 2009, **1**, 107-110.
37. T. R. Carlson, J. Jae, Y.-C. Lin, G. A. Tompsett and G. W. Huber, *J. Catal.*, 2010, **270**, 110-124.
38. J. Jae, G. A. Tompsett, A. J. Foster, K. D. Hammond, S. M. Auerbach, R. F. Lobo and G. W. Huber, *J. Catal.*, 2011, **279**, 257-268.
39. S. A. Kalota and I. I. Rahmim, 2003.
40. J. Weitkamp and L. Puppe, *Catalysis and zeolites: fundamentals and applications*, Springer Science & Business Media, 1999.
41. Y. S. Prasad, N. N. Bakhshi, J. F. Mathews and R. L. Eager, *Can. J. Chem. Eng.*, 1986, **64**, 285-292.
42. J. D. Adjaye, R. K. Sharma and N. N. Bakhshi, in *Advances in thermochemical biomass conversion*, ed. A. V. Bridgwater, Blackie Academic & Professional, Glasgow, UK, 1994, vol. 2, pp. 1032-1046.
43. S. P. R. Katikaneni, J. D. Adjaye and N. N. Bakhshi, *Energy & Fuels*, 1995, **9**, 599-609.
44. J. C. Oudejans, P. F. Van Den Oosterkamp and H. Van Bekkum, *Applied Catalysis*, 1982, **3**, 109-115.
45. C. J. Gilbert, J. S. Espindola, W. C. Conner, J. O. Trierweiler and G. W. Huber, *Chemcatchem*, 2014, **6**, 2497-2500.
46. F. Ates, A. E. Putun and E. Putun, *J. Anal. Appl. Pyrolysis*, 2005, **73**, 299-304.
47. E. Putun, F. Ates and A. E. Putun, *Fuel*, 2008, **87**, 815-824.
48. E. Kantarelis, W. Yang and W. Blasiak, *Energy & Fuels*, 2014, **28**, 591-599.
49. E. Putun, B. B. Uzun and A. E. Putun, *Biomass Bioenerg.*, 2006, **30**, 592-598.
50. E. Kantarelis, W. Yang and W. Blasiak, *Fuel*, 2014, **122**, 119-125.
51. H. Yang, R. J. Coolman, P. Karanjkar, H. Wang, Z. Xu, H. Chen, T. J. Moutziaris and G. W. Huber, *Green Chemistry*, 2015.
52. J. L. Motz, H. Heinichen and W. F. Hölderich, *J. Mol. Catal. A: Chem.*, 1998, **136**, 175-184.
53. M. Gubelmann and P.-J. Tirel, Google Patents, 1991.
54. G. I. Panov, A. S. Kharitonov and V. I. Sobolev, *Applied Catalysis a-General*, 1993, **98**, 1-20.
55. V. Zholobenko, *Mendeleev Commun.*, 1993, 28-29.
56. V. L. Zholobenko, I. N. Senchenya, L. M. Kustov and V. B. Kazanskii, *Kinet. Catal.*, 1991, **32**, 132-137.
57. P. R. Makgwane and S. S. Ray, *J. Mol. Catal. A: Chem.*, 2015, **398**, 149-157.
58. D. Baykan and N. A. Oztas, *Mater. Res. Bull.*, 2015, **64**, 294-300.

59. C. Wang, L. Hu, Y. Hu, Y. Ren, X. Chen, B. Yue and H. He, *Catal. Commun.*, 2015, **68**, 1-5.
60. C. Mukarakate, X. Zhang, A. R. Stanton, D. J. Robichaud, P. N. Ciesielski, K. Malhotra, B. S. Donohoe, E. Gjersing, R. J. Evans, D. S. Heroux, R. Richards, K. Iisa and M. R. Nimlos, *Green Chemistry*, 2014, **16**, 1444-1461.
61. H.-m. Chang, B. Cowling Ellis and W. Brown, in *Holzforschung - International Journal of the Biology, Chemistry, Physics and Technology of Wood*, 1975, vol. 29, p. 153.
62. S. Czernik, R. French, A. Stanton and K. Iisa, NREL Milestone Report, 2012, p. 12.
63. R. J. Evans and T. A. Milne, *Energy Fuels*, 1987, **1**, 311-319.
64. M. W. Jarvis, T. J. Haas, B. S. Donohoe, J. W. Daily, K. R. Gaston, W. J. Frederick and M. R. Nimlos, *Energy Fuels*, 2011, **25**, 324-336.
65. A. Aho, N. Kumar, K. Eranen, T. Salmi, M. Hupa and D. Y. Murzin, *Fuel*, 2008, **87**, 2493-2501.
66. K. Hemelsoet, J. Van der Mynsbrugge, K. De Wispelaere, M. Waroquier and V. Van Speybroeck, *Chemphyschem*, 2013, **14**, 1526-1545.
67. D. Lesthaeghe, A. Horré, M. Waroquier, G. B. Marin and V. Van Speybroeck, *Chemistry – A European Journal*, 2009, **15**, 10803-10808.
68. C. Mukarakate, A. M. Scheer, D. J. Robichaud, M. W. Jarvis, D. E. David, G. B. Ellison, M. R. Nimlos and M. F. Davis, *Rev. Sci. Instrum.*, 2011, **82**.
69. M. Saidi, F. Samimi, D. Karimipourfard, T. Nimmanwudipong, B. C. Gates and M. R. Rahimpour, *Energy Environ. Sci.*, 2014, **7**, 103-129.
70. J. F. Haw, *Phys. Chem. Chem. Phys.*, 2002, **4**, 5431-5441.
71. W. Wang and M. Hunger, *Acc. Chem. Res.*, 2008, **41**, 895-904.
72. R. Von Ballmoos and W. M. Meier, *The Journal of Physical Chemistry*, 1982, **86**, 2698-2700.
73. A. Corma, J. Mengual and P. J. Miguel, *Applied Catalysis A: General*, 2012, **421-422**, 121-134.